^{222}Rn study throughout different seismotectonical areas: comparison between different techniques for discrete monitoring

Carlo Mancini ([1]), **Fedora Quattrocchi** ([2]), **Claudio Guadoni** ([1]), **Luca Pizzino** ([2]) **and Benedetto Porfidia** ([2])
([1]) *Dipartimento Ingegneria Nucleare (DINCE), Università di Roma «La Sapienza», Roma, Italy*
([2]) *Istituto Nazionale di Geofisica, Roma, Italy*

Abstract
In the frame of the geochemical monitoring of seismicity mainly aimed at deepening the relationships between active seismotectonics and fluid geochemistry, *i.e.* earthquake prediction, a ^{222}Rn study was accomplished. It is addressed to inter-calibrate in diverse tectonic settings different methods to measure radon in groundwater: Alpha Scintillation Method using Lucas Cells (ASM-LCC) and Gamma Spectrometry Method (GSM), adopting both the Charcoal Trap Method (CTM) by Active Charcoals Canisters (ACC) and the Beaker Marinelli (BM) sampling devices. The intercalibration occurred on the field as well as in the laboratory, to finally select the best-fitting to gather radon information in each situation. Three Italian areas were selected to verify radon behavior and background concentration in different seismotectonical, geo-structural and lithological settings: ancient metamorphosed rocks – quiescent faults (Eastern Alps), carbonate foreland – active faults (Gargano) and quiescent volcanic structure overlapping a carbonate basement – swarm seismic activity (Colli Albani). The high radon concentration variability and the factors affecting radon behavior in groundwater (*i.e.* carrier gases presence, convection along fault systems, lithology influence, etc.) strongly constrain the measurement method to be adopted. The results point out apparently that the ASM-LCC method may be useful for expeditious and quick response of groundwater radon concentration during geochemical surveys aimed at grossly detecting the presence of tectonic structures, the deepening of circulation or the peculiar geological features linked to the presence of U-Th minerals. This method is not reliable for accurate measurements, while the GSM methods showed low standard deviation (higher precision with respect ASM-LCC) and accurate radon measurements. Finally, a customized DINCE Standard Radiactive Source (DSRS) was set up, and first used for the efficient estimation of the ING available Lucas Cells. A calibration factor for each ING Lucas Cell was defined and the most critical aspects of the ASM-LCC method revised.

Key words *radon in groundwater versus seismotectonics – ASM-LCC and GSM methods – Eastern Alps – Gargano – Colli Albani*

Mailing address: Dr. Fedora Quattrocchi, Istituto Nazionale di Geofisica, Via di Vigna Murata 605, 00143 Roma, Italy; e-mail: quattrocchi@ing750.ingrm.it

1. Introduction

Starting from the need of the ING geochemical research group to refine and cross-check the radon measuring method used during spatial and temporal monitoring throughout seismogenic areas, the DINCE laboratory made available its own radon measuring methods, standard sources and calibration devices, refined or newly customized for this specific inter-calibration test.

The radon measuring method for discrete monitoring adopted by ING is the Alpha Scintillation Method using Lucas Cells (ASM-LCC method in the text), that was proved, since the beginning of monitoring, to measure radon gas without precision and accuracy. Starting from this evidence, only an inter-calibration test may have been useful to clarify in a quantitative way the ASM-LCC method failings, despite the noteworthy fitness of the method during expeditious geochemical surveying, addressed to seismotectonical and hydrogeological studies (Quattrocchi and Calcara, 1998; Quattrocchi *et al.*, 1998, 2000a; Lombardi *et al.*, 1999; Salvi *et al.*, 2000).

The Gamma Spectrometry method (GSM method in the text) was adopted and standardized by DINCE, using both the Charcoal Trap Method (CTM) by means of newly standardized Active Charcoal Collectors (ACC) and the Beaker Marinelli (BM) sampling devices. It has proved as accurate and moderately sensitive method (Belloni *et al.*, 1995).

This work started with the aim of verifying the possibility to adopt on the field the two methods together in a sort of parallel radon surveying, because of the quickness and readiness of the ASM-LCC measure and conversely the more accurate but delayed GSM measure.

This ^{222}Rn study should also be a prerequisite for the future development of the collaboration between ING and DINCE regarding the assembly and standardization of different methods for continuous radon monitoring (Quattrocchi *et al.*, 1997; Galli *et al.*, 2000), addressed to environmental and natural risk assessment (seismic, volcanic and chemical hazards, *i.e.* radon indoor).

This need arises from state-of-the-art knowledge on the strict relationships between fluid geochemistry and seismotectonics (Toutain and Baubron, 1999) and from the ING surveillance requirements, *i.e.* to set up a proper geochemical surveillance network, using the completed GMS II prototype (Geochemical Monitoring System, Quattrocchi *et al.*, 2000b).

State-of-the-art earthquake prediction, using geochemical methods too, strongly recommends the definitive strategy of continuous monitoring instead of the discrete one (Igarashi *et al.*, 1995; Lombardi *et al.*, 1999; Toutain and Baubron, 1999; Quattrocchi *et al.*, 2000b).

The increasingly evident links between fluids and seismotectonical active processes (Sibson *et al.*, 1975, 1996; Nur and Walder, 1992; Fournier, 1991; Quattrocchi, 1999) warrant studies on the evolution of pore-pressure at depth, adopting – at surface – monitoring methods that may indirectly give information about the pore-pressure state within the Earth crust: radon monitoring has proved a very useful method to discriminate this kind of processes (Quattrocchi and Calcara, 1998; Quattrocchi *et al.*, 1998, 2000a; Lombardi *et al.*, 1999; Quattrocchi, 1999).

2. Radon as seismic precursor, geologic structures tracer and Rn-Indoor prone-areas location tool

The rationale driving the geochemical monitoring of natural fluids aimed at earthquake prediction studies and active fault recognition is mainly that the earthquake-related stress/strain changes may cause pore-pressure variations, which may, in turn, affect the fluid-rock interaction and fluid migration mechanisms, particularly along pervious faults, that may be defined as geochemically active faults (Lombardi *et al.*, 1999; Salvi *et al.*, 2000).

Fault system and geologic structure recognition by radon also constitute a basis for the recently exploited problem of the definition of the prone-areas to assess the Rn-indoor risk (Pizzino *et al.*, 1999).

Radon, helium, carbon dioxide, methane, mercury and several other volatile species have been found generally to have anomalous concentrations along «active» faults, suggesting that faults may be paths of least resistance for the terrestrial gases generated or stored in the Earth to escape to the atmosphere (see after King 1986; Quattrocchi *et al.*, 1999).

It is accepted almost worldwide that radon surveying either in groundwater or in soil gas may be a very helpful methodology to search for buried-active faults and U-rich bodies (Hauksson, 1981; King *et al.*, 1986; Toutain and Baubron, 1999). Particular emphasis has been

placed on this inert gas, due to many physico-chemical and fluid-dynamic intrinsic characteristics, rendering it very sound for earthquake prediction experiments and active fault recognition studies, as follows:

– Radon, as a member of the radioactive decay series of uranium, exists ubiquitously in crustal rocks, allowing very widespread radon monitoring method despite the fact that normally it is found in trace amounts in fluids. Moreover, in different geodynamical settings the lithologic signature of radon may be discriminated from the tectonic one (Torgersen *et al.*, 1990; King *et al.*, 1993; Quattrocchi *et al.*, 1999; Lombardi *et al.*, 1999).

– Radon is of most geophysical interest because of both its high mobility in the crustal environment, moving through pore fluids by different mechanisms, *i.e.* diffusion, convection, bubbling carrier gases (after Schroeder *et al.*, 1965; Thomas, 1988; Quattrocchi *et al.*, 1999) and its emission from a crustal rock/region related to the ongoing stress/strain field (after Giardini, 1976; Holub and Brady, 1981; Igarashi and Wakita, 1995; Igarashi *et al.*, 1995).

Too many efforts have been addressed to discrete monitoring instead of the continuous one, with few exceptions (Noguchi and Wakita, 1977; Friedmann and Hernegger, 1978; Shapiro *et al.*, 1980; Friedmann, 1985; Galli *et al.*, 2000 and references herein). Up to date, the continuous monitoring efforts exploited in various countries have underestimated the importance of a fully multi-variable approach in designing networks in which radon data may be cross-correlated and discussed together with other geochemical and geophysical data (Honkura and Isikara, 1991; Quattrocchi and Calcara, 1998; Quattrocchi *et al.*, 2000b).

The observed temporal Rn anomalies may assume either a spike-like (lasting less than a day/few hours) or a continuous long/medium term anomalous shape, generally depending on the distance of the impending earthquake, although reliable geochemistry earthquake prediction algorithms do not yet exist (Hauksson, 1981; Etiope *et al.*, 1997; Toutain and Baubron, 1999).

A «sensitive» site selection is the prerequisite to accomplish good results: the choice generally falls along «active» faults or at the crossing point of different ones as well as in the vicinity of deep gas gushing sites (Quattrocchi and Venanzi, 1989; Wakita *et al.*, 1989; Quattrocchi and Calcara, 1998; Quattrocchi *et al.*, 1999; Lombardi *et al.*, 1999). The non-tectonically induced variations must be carefully eliminated in search of earthquake-related anomalies (Wakita *et al.*, 1989; Virk and Baljinder, 1993).

As regards the most probable mechanisms generating the radon – and other gases – anomalies, the wide existing literature stressed the role of pre-failure inelastic volume increase because of development of cracks and of episodic upward migration of deep seated gases driven by extensive stress field – *i.e.* Fault Valve Activity mechanism and/or phase separation – (Scholz *et al.*, 1973; Sibson *et al.*, 1975, 1996; Fyfe *et al.*, 1978; Fournier, 1987, 1991; Nur and Walder, 1992; Quattrocchi and Calcara, 1998; Quattrocchi, 1999).

3. Methods

Among the possible methods to measure ^{222}Rn concentration in water either by discrete or continuous mode (*i.e.* by a method giving measures every minutes/hours), we have taken into consideration two of them: the Alpha Scintillation Method by Lucas Cell Counting (ASM-LCC) and Gamma Spectrometry Method (GSM), that seem to be the most effective for our purposes. These methods are essentially based on the detection of the radiation emitted by radon's decay products. As shown in table I, isotopes of polonium, *i.e.* ^{218}Po and ^{214}Po, both are α-particle emitters, whilst ^{214}Pb and ^{214}Bi decay by emission of β and γ radiation of different energies. The two methods discussed below are based on the detection of α and γ radiation, respectively.

The four nuclides of the ^{238}U series, having much shorter half lives in comparison with ^{222}Rn, so that secular equilibrium will be reached within about 200 min, are: ^{218}Po, ^{214}Pb, ^{214}Bi and ^{214}Po. Table I summarizes the main characteristics of ^{222}Rn and the nuclides originated by radon decay, from ^{218}Po to the stable ^{206}Pb.

Table. I. Main characteristics of ^{222}Rn and its «decay products».

Radionuclide	Historical name	$T_{1/2}$	Main emission energies (MeV)		
			Alpha	Beta	Gamma
^{222}Rn	Radon	3.823 d	5.49		
^{218}Po	Radium A	3.05 min	6.00		
^{214}Pb	Radium B	26.8 min		0.67	0.242 (8%)
				0.73	0.295 (19%)
				1.02	0.352 (37%)
^{214}Bi	Radium C	19.7 min		1.00	0.609 (46%)
				1.51	1.120 (15%)
				3.26	1.764 (16%)
^{214}Po	Radium C′	164 ms	7.69		
^{210}Pb	Radium D	22.3 y		0.015	
				0.061	
^{210}Bi	Radium E	5.01 d		1.161	
^{210}Po	Radium F	138.4 d	5.305		
^{206}Pb	Radium G	Stable			

3.1. *Alpha Scintillation Method by Lucas Cells (ASM-LCC)*

The ASM-LCC method has been widely used to date, in different customized devices, deserving special interest for continuous monitoring applied to geochemical surveillance of seismicity (Nogouchi and Wakita, 1977; Quattrocchi *et al.*, 1997; Galli *et al.*, 2000 and references herein) and for discrete surveying (Quattrocchi *et al.*, 1998; Lombardi *et al.*, 1999; Salvi *et al.*, 2000).

The ^{222}Rn concentration measurements accomplished by this method need the presence of the well-known cylindrical scintillation flask called Lucas Cell. ING selected the instrumentation produced by EDA Instruments Inc.™ (4 Thorncliffe Park Drive, Toronto, Canada, M4H 1H1) with Lucas Cell of Pylon type (Pylon Electronics Inc.™, 147 Colonnade Road, Ottawa, Ontario, K2E 7LR), having a volume of 125 cm^3, and two-way Swagelok™ plugs.

The measures may be performed starting from liquid or gaseous phases (springs, wells, gaseous discharges, fumaroles, gas pools, etc.): starting from groundwater a stripping device acting under vacuum is needed to extract the gaseous phase from water, subsequently analyzed by the photo-multiplier (RU200 and EDA RD200 EDA Instruments Inc.™ units respectively). The water-stripping standard cylindrical glass vial is fitted to the base of a thin diffusion disk-filter allowing gas-stripping from water. Recently it was replaced by a DINCE customized one, having the same volume, and fitted with a hermetic closure threaded plastic cap, improving handling on the field and cutting air contamination. The kind of diffusion disk-filter used significantly affects stripping efficiency (mean value of 75%) and precision as detailed later.

The final algorithms used by ING to calculate the ^{222}Rn concentration (pCi/L readily converted in Bq/L by dividing for 27.04), by considering the available EDA Instruments Inc.™ instrumentation, are

$$IF_{(water)} = \\ = 1000_{(cm^3/L)} \times 1/3.6_{(pCi/cpm)} \times 100/75 \times 1/120_{(1/cm^3)} = 3.0 \quad (3.1)$$

$$IF_{(gas)} = 1000_{(cm^3/L)} \times 1/3.6_{(pCi/cpm)}\ 1/125_{(1/cm^3)} = 2.2 \quad (3.2)$$

$$[^{222}Rn]_{(pCi/L,\ water)} = (IF_{(water)} \times rt_{(cpm)}) \times 2.91208/TF \quad (3.3)$$

$$[^{222}Rn]_{(pCi/L,\ gas)} = (IF_{(gas)} \times rt_{(cpm)}) \times 2.91208/TF \quad (3.4)$$

where $IF_{(water)}$ and $IF_{(gas)}$ are the «Instrumental Factors» for water and gas phases respectively; rt is the average reading (on 3-4 data reading by photo-multiplier, with 1 min time selection) at time $t_{(hours)}$, expressed in counts per minutes (cpm). TF is the «Temporal Factor» depending on the difference between t and the equilibrium time (4 h after sampling); TF is equal to 1.0 if $t = 4.0$ h. The TF values tables have been calculated starting from the decay curve of ^{222}Rn and its daughters. These tables are available from EDA Instruments Inc.™ technical specifications. Here, $1/3.6_{(cpm/pCi)}$ is specified as sensitivity: 1 pCi/L corresponds to 3.6 cpm; 0.75 derives from the 75% stripping efficiency of the system as a whole (RU200 Unit); the 120 cm^3 is the volume of the water glass vial; the 125 cm^3 is the volume of the LCC.

The radon measure is readily available only a few hours after sampling, also having gross radon information a few minutes after sampling. This pre-requisite may be considered the main advantage of this method.

3.2. *Gamma Spectrometry Method (GSM)*

The GSM method, although not as widespread as the ASM method, offers many advantages, that make it one of the most versatile and reliable methods for groundwater ^{222}Rn concentration measurements, both in groundwater and in soils/indoors. It consists of specific radon activity measurement by detecting the γ radiation coming from the radon decay products ^{214}Pb and ^{214}Bi, once secular equilibrium with the parent radon is reached. The impulses from the photo-multiplier, suitably amplified, pass through both a window discriminator and a rate counting: the rate of counts – multiplied by a calibration factor – obtained using a known activity sample, allows the value of radon concentration to be inferred for each sample.

The GSM method may be engaged, both by using the water sample directly and by extracting the gas phase from the liquid one, by air stripping before the measurement. In the first case, special vials were adopted, called Marinelli Beaker (BM), while in the second case, the Charcoal Trap Method (CTM) was employed adopting customized ACC.

3.2.1. The Beaker Marinelli (BM) device

The BM, filled with the water sample was manufactured as a cylindrical polyethylene-methacrylate vial, with a 8 cm diameter cylindrical cavity; at the lower base, the cavity allows the priming of a 3″ photo-multiplier tube, increasing the detection efficiency.

Starting from the original version of the BM module, shown in fig. 1, a few minor modifications have been added. To date different options of BM are available; the volume varies from a minimum of 950 cc to a maximum of 1065 cc. All the prototypes had a hermetic closure using o-rings, so that a slight pressure within the sampled water was easily created, once filled under flux. In this connection, care should be taken to make at least one complete refilling of the BM volume, during the water sampling, avoiding – at the same time – bubble formation after the closure of the vial, which may impair measurements. The BM-photo-multiplier assembly must be sufficiently shielded to avoid as much as possible the contribution of the background γ radiation: a specific study aimed at optimizing the shielding of the device was accomplished, yielding the final design of a low-background lead pellets cylindrical shield-well whose section is shown on fig. 1, displaying the coupling between the BM and photo-multiplier; the thickness of the shielded walls was selected as about 7 cm, allowing an attenuation factor of the background γ radiation equal to 0.02.

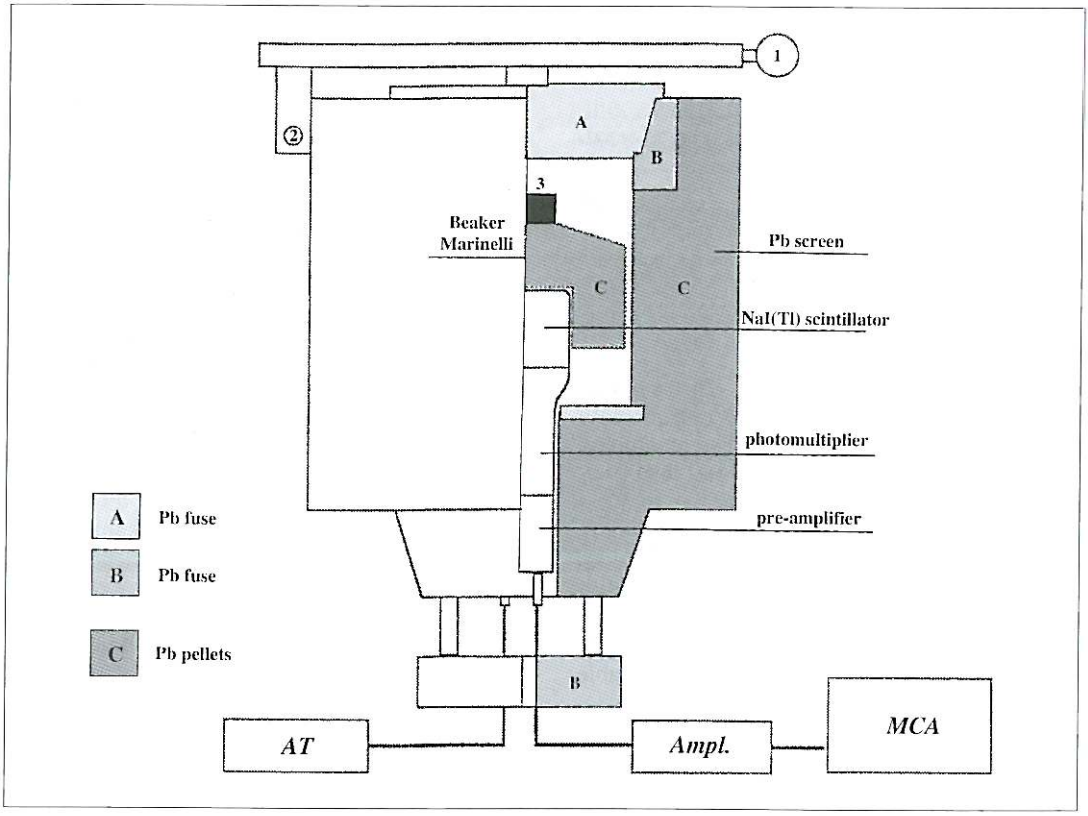

Fig. 1. Beaker Marinelli (BM) coupled with a γ spectrometer, assembled by DINCE. 1 = Cap lever; 2 = hinge of the cap lever. AT is the High Voltage supply, AMPL is the spectroscopy amplifier, MCA is the Multi-Channel Analyser (MCA).

3.2.2. Charcoal Trap Method using Active Charcoal Collectors (CTM-ACC)

The GSM method coupled with the CTM is based on the capability of charcoal soundly treated to absorb radon gas. Indeed, because of the dry-distillation process using both animal or vegetable residues in a range of temperature spanning from 400 °C to 600 °C, a porous charcoal substratum was obtained, further activated by phosphoric acid-zinc chloride treatment, acting as graphytising catalysts.

The absorption was ruled by Henry's law:

$$v = k \cdot p$$

in which the gas volume, v, is the adsorbed gas for each mass unit of charcoal, p is the partial pressure and k is the adsorption coefficient. Typical values of the adsorption coefficient are 4000 Bq for each gram of active charcoals, for each Bq/cm^3 of radon in air. The charcoal was inserted within metallic cylindrical boxes, with a variable diameter, spanning between 6 and 10 cm, so called collectors or canisters, thus defined Active Charcoal Collectors (ACC). Each collector contains a range of 25-100 grams of active charcoal, filling a stratum 2 cm thick. The collector may be re-used after heating within a temperature range of $100 \div 120$ °C, for an interval of more than 10 h, to get rid of the existing residues.

The measurements of radon concentration in water, accomplished by CTM-ACC, are performed by transferring the extracted gas from water to the charcoal itself (fig. 2). It is accomplished adopting a similar procedure as that used for the ASM-LCC method: by engaging a small pump (Q ≅ 2,5 l/min), a precise aliquot of air re-circulates for a fixed time interval (normally optimized spanning from 2 to 5 min, depending on the water volume and on the diffusion filter characteristics) within sampled water.

Initially, in the laboratory, traditional ACC – 12 cm diameter wide – have been used; later, a second type of ACC was developed, adopting a 6 cm diameter width, taking into consideration some advantages gained with respect to the first type. For water filling, special glass bottles (0.598 liter volume) were used; one of these bottles is shown in fig. 2 together with the degassing circuit unit. The latter, called «re-circulation unit», was placed within a small case, customized in laboratory, allowing easy transport as well an easy recharging of the internal battery, supporting both the pump power and a regulation timer, conceived for managing the re-circulation time (fig. 2). A similar configuration was developed for «enrichment» of the new ACC type. The bottles were fitted with two inlets and a cap, which are closed soon after sampling. The first was connected to a candle type diffusion disk-filter – placed at 0.5 cm from the

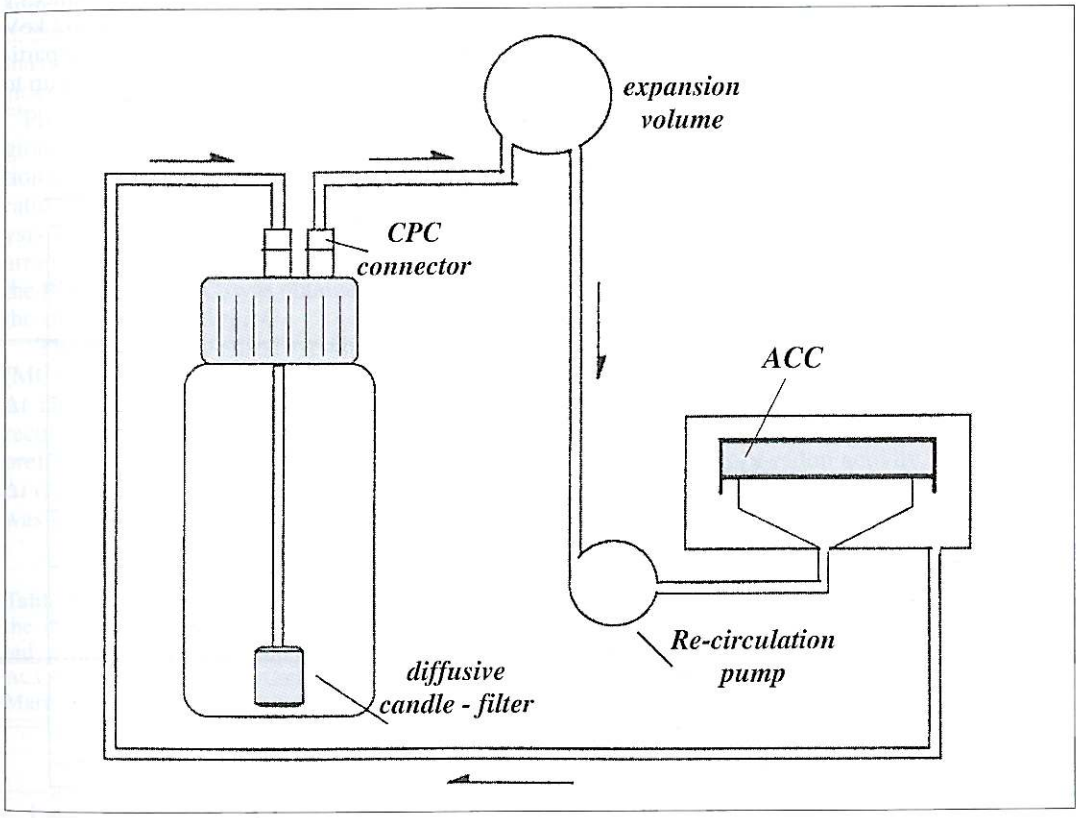

Fig. 2. Scheme of the re-circulation unit, assembled by DINCE, used coupled with the Active Charcoal Collector (ACC) samplers. CPC connector are hydraulic click connectors.

bottom of the vial – used for air re-circulation during the degassing phase, while the second allows the outlet of the air enriched in radon, before reaching the ACC. Each the inlets have CPC quick-plug connectors (hydraulic click connectors).

The ACC, not very bulky and relatively lighter than the Lucas Cells, may be easily transferred in the laboratory by cai-post from remote surveying, for the γ spectrometric analyses.

It is much easier to transport a certain number of ACC, with respect to as many water filled BM, especially in the case of a huge number of samples to be collected.

3.3.3. Instrumental assembly and final concentration algorithms

The GSM instrumental assembly used for the laboratory radon measurements is made up of the following components (fig. 1):

– NaI(Tl) scintillation crystal (dimension: $3'' \times 3''$, Bycron™), coupled with a photo-multiplier, endowed with a pre-amplifier.

– High voltage supply (Silena™, Mod. 7712) pre-set normally on 825 V.

– Spectroscopy amplifier (Silena™, Mod. 7612L), with maximum gain equal to 20.

– Multi-channel analyzer (Silena™, Mod. Cato), with 4096 channels.

– Power continuity group, on-line allowing voltage stability.

– Low-background lead balls cylindrical screen-well, 7 cm thick.

– If necessary, portable case, re-circulation unit equipped for radon transfer to the ACC (CTM).

As mentioned above, the radon decay products, which decay with γ emission, are ^{214}Pb and ^{214}Bi radio-nuclides. The first mostly produces γ radiation with energy of 242, 295 and 352 keV respectively, while the second produces γ particles with an energetic spectrum spanning up to

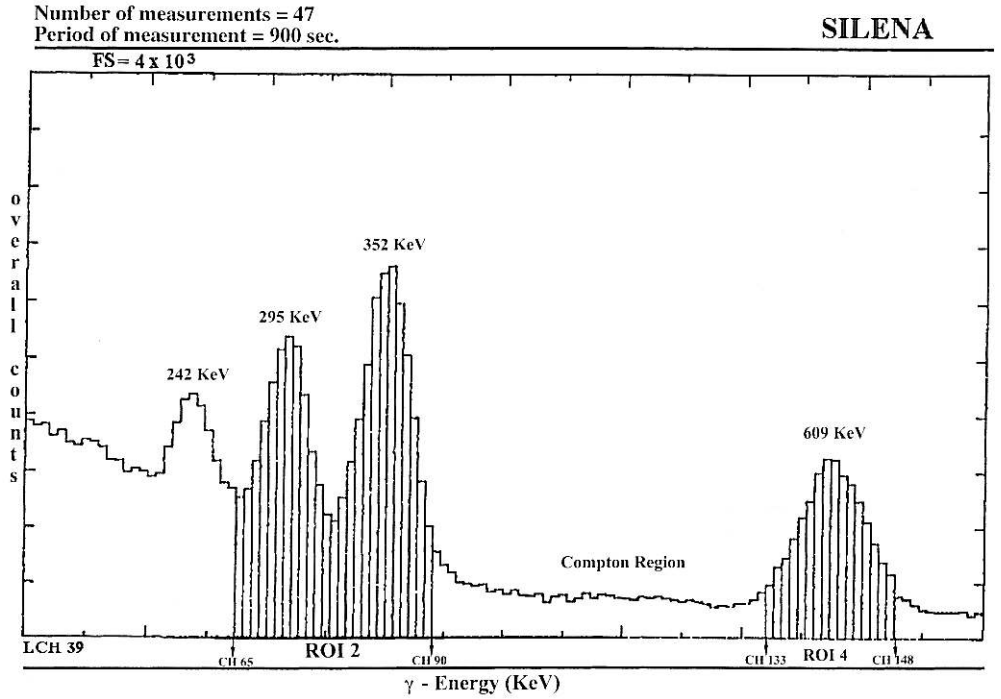

Fig. 3. Typical γ-spectrum visualised by the MCA, used by DINCE.

2 MeV; the most probable energy is 609 keV (table I, fig. 3).

The Multi-Channel Analyzer (MCA) receives as input the amplified impulses and then produces as output a γ spectrum, as shown in fig. 3, which points out three peaks relative to Pb and Bi isotopes. The MCA was set for 1/4 of the total number of the available channels (1024 channels). In the final measurement performance the ^{214}Pb peaks of 295 and 352 keV were taken into consideration, as well as the ^{214}Bi peak of 609 keV, that were between channels 65 and 90, as well as between channels 133 and 148, respectively. The two mentioned intervals are indicated as *roi 2* and *roi 4* (*roi* = region of interest, fig. 3), while the specified *roi 1* and *roi 3* are the channel intervals relative to the ^{214}Pb-242 keV and the ^{214}Bi-Compton Region, respectively. The signal/background ratios, analyzed as a function of the integration intervals (*rois*) showed that the maximum value was obtained taking into consideration just *roi 2* and *roi 4*. In fact the peak of ^{214}Pb-242 keV (*roi 1*) and the Bi-Compton Region (*roi 3*) did not give an appreciable contribution to the signal, the latter further worsening the ratio. Table II summarizes the results of an analysis of the S^2/B ratios, relative to different *roi* arrangements: the maximum value, using both the BM and the ACC, was obtained, considering the sum of *roi 2* and *roi 4*.

The MCA may be used even in a Multiscaler (MCS) mode: in this case, once a time interval Δt and a sound *roi* are fixed, the instrument records the counting integral extended to the prefixed *roi*, for each consecutive time interval Δt (*i.e.* 900 s). In the MCS mode, a specific *roi* was established between channels 64 and 152.

Table II. S^2 (signal) / B (noise) ratio normalised to the maximum value, for the different *rois* selected within the Multi-Channel Analyser (MCA). ACC = Active Charcoals Canisters, BM = Beaker Marinelli.

Roi	S^2/B ACC	S^2/B BM
1 + 2 + 3 + 4	0.82	0.44
2 + 3 + 4	0.70	0.35
2 + 4	1.00	0.44

The addition of some channels to the boundaries of the *roi* (64 rather than 65, and 152 rather than 148) is advisable, to cut the counting noises due to the drifts of the electronic chain, which is always possible considering the MCS modality time intervals. Both for the MCA and MCS modalities of measurements, the counting time was fixed at 15 min.

The counting obtained by the integration on the pre-selected roi represents the sum of that effectively linked to the radon concentration within the sample plus the background counting; they were labeled, therefore, as gross counting (C). To calculate definitively the counting due to radon, defined as net counting (C_{net}), it was necessary to remove the background counting (C_B) from the gross counting. Moreover, radon decay, which occurs in a $T_{1/2}$ of 3,823 days, needed to be considered. Therefore, the datum relative to the measuring time must be corrected, to go back to the sampling time; the correction was obtained by dividing the obtained counting by a factor, called Decay Factor (DF). DF was calculated by the algorithm

$$DF = \exp\left[-\frac{0.693}{5501}\cdot t\right]$$

in which t is the elapsed time (minutes) between the sampling time and the measuring time, while 5501 is the radon $T_{1/2}$ (expressed in minutes). The number of countings, obtained by dividing the net counting, by the DF, represents the corrected counting (C_c). To translate the number of counts in terms of radon activity, it was necessary to calibrate the system as a whole, using a standard (fixed activity source); dividing the number of counts revealed using that standard, by the activity itself, a Calibration Factor (E) was obtained, expressed as counting/Bq. The radon activity of the sample will be, therefore, equal to the ratio between the corrected counting (C_c) divided by the Calibration Factor (E).

If it is necessary to calculate the activity concentration (expressed as Bq/l), we need to divide the formerly obtained datum, either by the volume of the used BM, or by the volume of the glass-bottle (expressed in liters), when the measurement was obtained with the CTM-ACC method, presuming a degassing efficiency equal

to 1.00 (H.F. Lucas). This process may be described by the formula

$$A = \frac{C - C_B}{DF \cdot E \cdot V}$$

where V is the initially sampled water volume, A is the radon activity expressed in Bq/L. As the calibration was performed by a specific-known activity collector, the last formula is valid – strictly speaking – only in the case accomplished with the CTM-ACC method. If the measurement is accomplished by a BM, the counting efficiency of the latter must be considered with respect to the CTM. Therefore, a factor F_{bc} was defined that expresses the ratio between the counting frequency recorded for a BM and the one recorded for the same CTM-ACC activity. Therefore the previous formula was modified as follows, using the BM device:

$$A = \frac{C - C_B}{DF \cdot E \cdot V \cdot F_{bc}}.$$

The product $E_{bM} = E \cdot F_{bc}$ represents directly the Calibration Factor relative to the BM. Table III summarizes the characteristic parameters relative to the BM as well as to the CTM-ACC, inferred on the basis of a huge number of measures.

4. Results

4.1. *Discrete radon monitoring over different areas*

Three areas were selected to perform radon surveying in different geodynamical conditions, *i.e.*, diverse radon concentration and affecting factors, to check the reliability of the two methods exploited together and to discriminate the potentiality, disadvantages and failings of each method in different settings.

The three areas differ from seismotectonical, geo-structural and lithological points of view: ancient metamorphosed rocks – quiescent faults (Eastern Alps), carbonate foreland – active faults (Gargano) and a quiescent volcanic structure overlapping a carbonate basement – swarm seismic activity (Colli Albani).

Table III. Standard counting (units: count per 900 s) and background level measured for the Active Charcoal Collectors (ACC) and for the Beaker Marinelli (BM).

Method	Roi 1 ch: 53-63	Roi 2 ch: 65-90	Roi 3 ch: 92-128	Roi 4 ch: 130-145
ACC standard 308 Bq	7237	24316	6423	8886
	7316	24321	6480	8828
Mean value	7277	24319	6452	8857
Net countings (S)	6498	22833	4548	8196
BM standard 305 Bq	7207	18678	5985	6563
	7069	18782	6029	6462
Mean value	7138	18730	6007	6513
Net countings (S)	6173	16882	4069	5748
Background with ACC	827	1509	1915	664
	731	1462	1892	659
Mean value (B)	779	1486	1904	662
Background with BM	991	1827	1933	787
	939	1870	1944	743
Mean value (B)	965	1849	1939	765

4.1.1. The Tonale-Pejo-Giudicarie fault systems survey (Eastern Alps)

The presence of gaseous mineral springs, often highly radioactive, throughout the Eastern Alps has been known for many years, but only recently was the strict link between the tectonic settings and their location was studied in detail by the collaboration between ING and the Earth Science Department of the University of Padua (Andreis, 1998; Danese, 1998 and references herein). In this work, fluid geochemistry and structural geology surveys during 1995 and 1996 were accomplished in the area (60 km × 70 km wide), comprising the tectonic lines of Tonale, Giudicarie, Pejo, Zebrù, Braulio and Slingia (fig. 4). Twenty-eight mineralized and eight oligo-mineral springs were collected during the 1995 survey, twenty during the 1996 survey (56 total samples). During the second survey, the radon concentration was measured in groundwater, using both the described methods: the ASM-LCC and the GSM coupled with the CTM-ACC. Besides radon content (table IV), we measured (ING unpublished data) physico-chemical parameters (temperature, pH, Eh, electrical conductivity), major elements and some minor and trace elements (CO_2, H_2S, NH_3, B, Li, SiO_2, Fe, Mn, Sr, F, Hg, As, etc.), useful to discriminate geothermal and tectonic-related deep fluid input and to understand the processes causing the radon enrichment in groundwater.

The area studied in this work is geodynamically very interesting to define the geochemical pathfinders of «quiescent» regional faults as the Giudicarie, Tonale and Pejo lines: almost all the gaseous ferruginous mineral springs are located

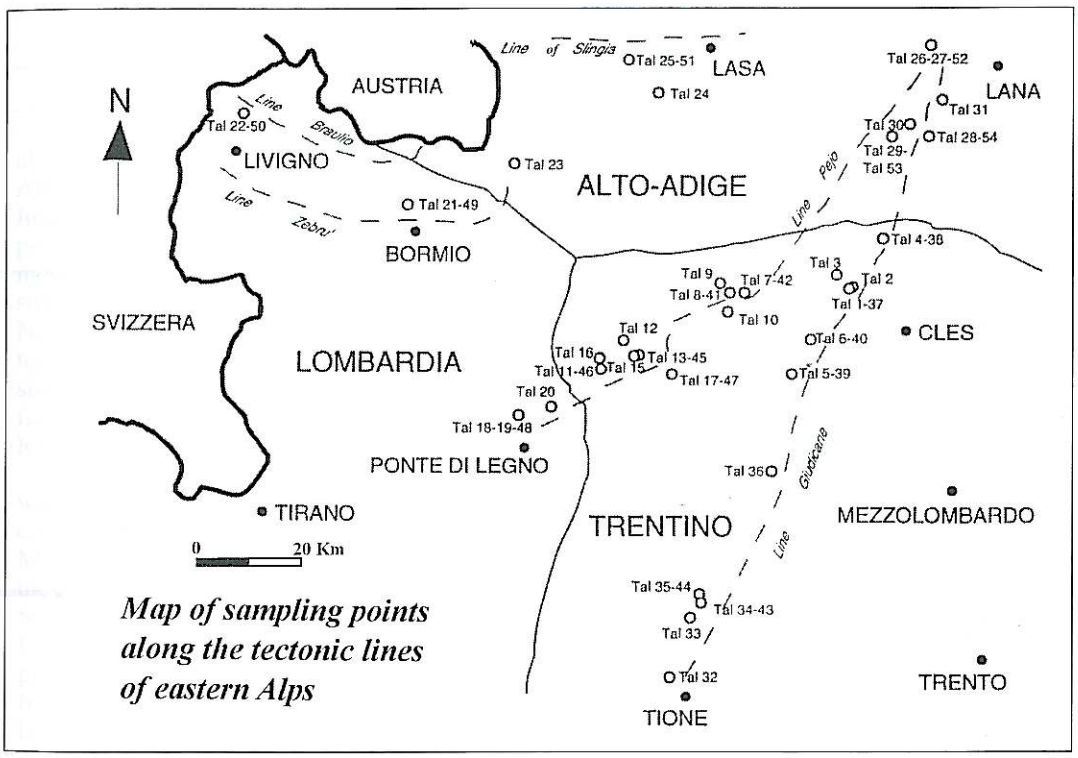

Fig. 4. Map of the sampling points along the tectonic lines of Eastern Alps (1996-1997 ING surveys). For TAL 40-54 both CTM and ASM-LCC methods inter-correlation have been accomplished.

Table IV. Results of the radon measurements carried out during the Gargano (11-15 July, 1996 and 3-13 August 1996) and Eastern Alps (18-31 July 1996) geochemical surveys. Nets counts are referred to: a 600 s interval for the samples GAR1-GAR18 and a 900 s interval for samples TAL 37-TAL 54. GC = Gamma Counting (GSM in the text); ACC = Active Charcoals Canisters; BM = Beaker Marinelli; LCC = Lucas Cell Counting.

Sample	Net counts	DF	Corrected counts	GC-ACC (Bq/L)	LCC (Bq/L)
GAR 1	973	0.489	1989	33	33
GAR 2	405	0.504	804	13	15
GAR 3	3257	0.512	6360	105	86
GAR 4	560	0.514	1089	18	27
GAR 15	892	0.700	1274	21	22
GAR 16	2417	0.704	3435	56	44
GAR 17	2950	0.714	4133	68	73
GAR 18	1257	0.723	1740	29	20
GAR 24	3	0.230	13	0	2
GAR 25	0	0.233	0	0	3
GAR 26	46	0.233	197	5	4
GAR 27	80	0.235	340	8	3
GAR 28	39	0.244	160	4	2
GAR 29	26	0.247	105	3	1
GAR 30	268	0.283	947	24	14
GAR 31	94	0.285	330	8	10
GAR 32	79	0.288	274	7	5
GAR 33	0	0.289	0	0	2
GAR 34	353	0.290	1217	30	17
GAR 35	388	0.330	1176	29	14
GAR 36	77	0.332	232	6	9
GAR 37	764	0.334	2287	57	27
GAR 38	118	0.337	350	9	15
GAR 39	43	0.340	126	3	3
GAR 40	186	0.342	544	14	6
GAR 41	124	0.343	362	9	6
GAR 42	94	0.277	339	8	6
GAR 43	86	0.278	309	8	4
GAR 44	34	0.279	122	3	3
GAR 45	8	0.280	29	1	1
GAR 46	0	0.281	0	0	3
GAR 47	284	0.330	861	21	9
GAR 48	308	0.337	914	23	10
GAR 49	104	0.338	308	8	6
GAR 50	51	0.339	150	4	2
GAR 51	299	0.340	879	22	11
GAR 52	3	0.390	8	0	1
GAR 53	245	0.397	617	15	7
TAL 37	259	0.271	956	16	8

Table IV (*continued*).

Sample	Net counts	DF	Corrected counts	GC-ACC (Bq/L)	LCC (Bq/L)
TAL 38	268	0.275	976	16	8
TAL 39	566	0.280	2019	33	15
TAL 40	296	0.283	1046	17	5
TAL 41	773	0.285	2716	45	15
TAL 42	806	0.318	2533	42	13
TAL 43	1634	0.546	2991	49	22
TAL 44	1389	0.549	2532	42	27
TAL 45	2027	0.566	3580	59	26
TAL 46	2605	0.572	4555	75	34
TAL 47	142	0.578	246	4	9
TAL 48	734	0.642	1144	19	7
TAL 49	59729	0.652	91550	1505	539
TAL 50	253	0.677	374	n.d.	481
TAL 51	1500	0.778	1929	32	10
TAL 52	162666	0.815	199494	3280	861
TAL 53	434	0.817	531	n.d.	276
TAL 54	2334	0.846	2758	45	89

along the regional lines bordering the Austro-Alpine Domain and the South-Alpine Domain. Inside the Austro-Alpine Domain there are important ductile and fragile fault zones (fig. 5), mostly characterized by transtensive mechanisms since the Upper Cretaceous period. During the Neogene age, the Alpine chain underwent intensive tectonics either strike-slip, or transtensive and transpressive, with high-angle faults formation, as the Tonale Line, the Pejo and the Rumo lines.

The Pejo Line is active (left trans-tensive, with eastward transport) spanning from Cretaceous to Miocene, between Ponte di Legno and Merano, with a SW-NE direction, representing the contact wall between the Ortles Nappe (Green Scists and gneiss facies) and the overlapping Ulten-Tonale Nappe (granulitic-amphibolitic pre-alpine facies). The actual N-S distensive fracture field involves high secondary permeability, the deepening of meteoric waters and the succeeding mineralized groundwater uprising along faults. Low-medium magnitude ($M < 4.0$) seismic events, concerning the Pejo Line, were recorded around Dimaro, Pejo, Rabbi and Bormio towns, with few historical events. Some events have been recorded in Val Rendena and the northern Val d'Ultimo.

The Tonale Line represents an important E-W segment (around 1 km wide fault zone) of the Periadriatic Line, extending from Valtellina to Val di Sole (Dimaro town), cut by the Giudicarie Line; its movement evolved in a right strike-slip tectonics during the Oligocene; further vertical movement, linked to the back-flexure of the Austroalpine Basement, re-started in the Neogene.

The Giudicarie Line (figs. 4 and 5) was clearly distinguished in a northern sector and in a southern sector, the first extended from Dimaro to Mules (Val d'Isarco), more studied in the present work. It belongs to the Periadriatic Line, trending NNE-SSW, as a marker of the left-lateral slip (around 70 km) of that regional line, between the Tonale Line and the Pusteria Line. The northern Giudicarie Line was active between the Upper Oligocene and Upper Miocene, although it seems linked to Permo-mesozoic tectonics.

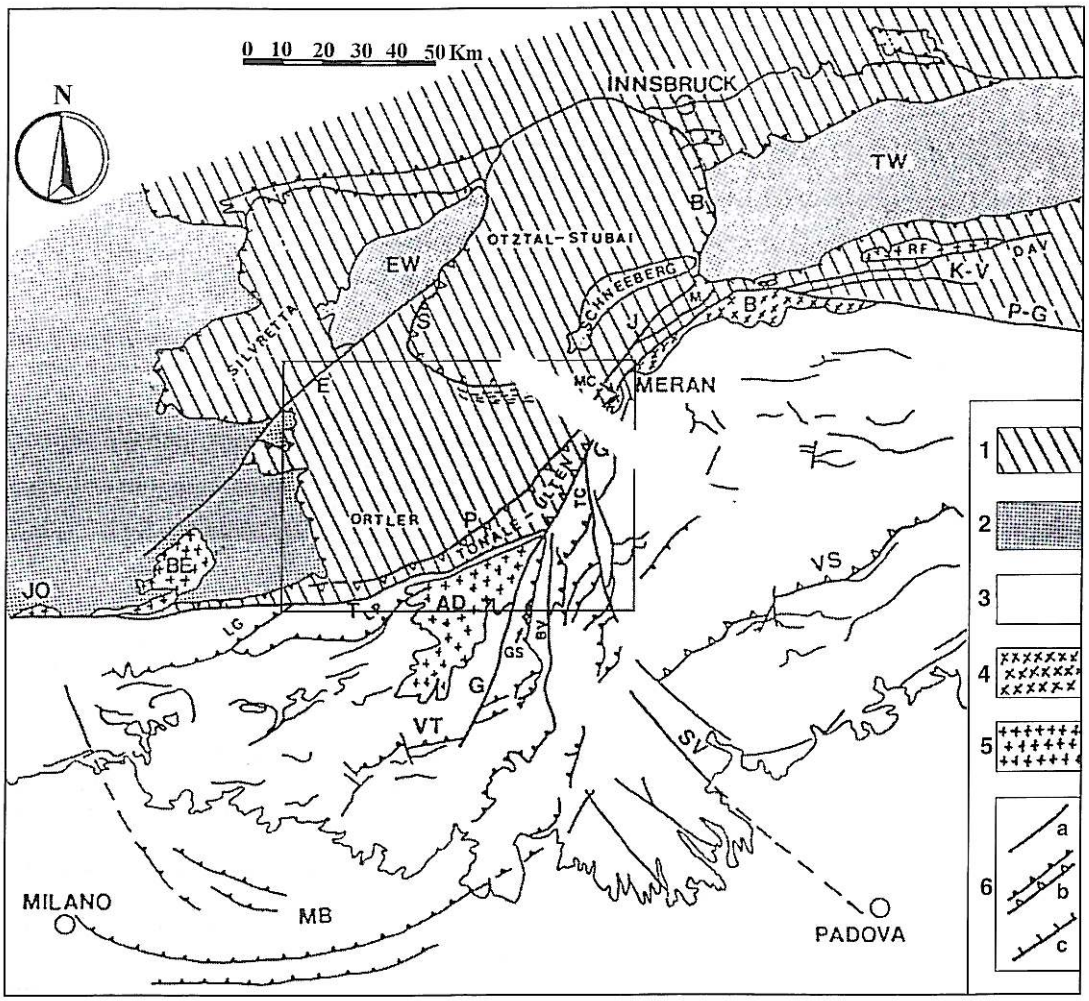

Fig. 5. Tectonic map of the central sector of the Southern Alps, including the Austro-Alpine and Pennidiche units of Eastern Alps (see Andreis, 1998; Danese, 1998, and references herein). 1 = Austro-Alpine system, including the Silvretta, Otztal-Stubai, Ortles and Tonale-Ultimo nappes; 2 = lower Austro-Alpine and Pennidiche nappes of the Err-Bernina system; 3 = Southern Alps; 4 = Permian intrusive bodies of Bressanone (B), Monte Croce (MC) and Sabion (GS); 5 = Tertiary magmatic bodies: Bregaglia (BE), Jorio (J), Adamello (AD) and Riesenferner (RF); 6 = faults (a), thrusts (b), normal faults (c). T = Tonale Line; E = Engadina Line; P = Pejo Line; G = Giudicarie Line; P-G = Pusteria-Gailtal Line; DAV = Defereggental-Antholz-Vals Line; KV = Kalckstein-Vallarga Line; S = Schlinig Thrust; B = Brennero Line; J = Jaufen Line; M = Mauls Line; EW = Engadina Window; TW = Tauri Window; TC = Trento-Cles Line; BV = Ballino-Vedretta dei Camosci Line; VT = Val Trompia Line; LP = Porcile Line; LG = Gallinera Line; MB = Milan belt; SV = Schio-Vicenza Line; VS = Valsugana Line. The selected area was interested by the 1996-1997 ING surveys.

The Braulio Line separates the Ortles Nappe from the Quatervals Nappe with an E-W very complex movement. The Zebrù Line with the same E-W trend direction spans from Shanf in Engadina to the «Passo del Zebrù» - Val Solda, representing the marker of the pre-oligocenic detachment between the Ortles Nappe and the crystalline basement.

The Slingia Line may be drawn from the Val Slingia to Piz Lat, separating the Otztal Nappe, at the top, from the basement and relative permo-mesozoic sedimentary covers.

Along these fault systems, the intensive fracture field allows the meteoric water to percolate in a deeper circulation, involving mineralized springs at surface.

In particular, along the Pejo Line 13 sampled mineral spring were aligned, while along the Giudicarie Line 12 mineral springs are located, with a NNE-SSW alignment. The Bormio thermo-mineral spring (TAL 21-49) is located along the western sector of the Zebru Line. The San Michele sulphureous spring (TAL 22-50) is located along the Braulio Line. The Lasa sulphureous spring is located near a cataclastic belt, attributable to the Slingia Line.

The Pejo Line mineralized groundwater is typically bicarbonate, either earth-alkaline (Pejo zone) or alkaline in the Rabbi zone, where a chlorine component has been discriminated (Fonte Antica Rabbi, TAL 7-42, up to 5 meq/L). The Val d'Ultimo springs also showed a Ca-sulfate composition (Uberrwasser and Lotterbad, TAL 29-53 and 30) as in the Miniera di Magnetite (TAL 17-47) mineralized spring, located along the Pejo Line.

The presence of a huge CO_2 flow within the mineralized springs involves enhanced aggressive water-rock interaction processes (pH around 5-6.5) with enrichment in solution of major, minor and trace elements (*i.e.* Rn, He, H_2S, Li, B, Fe, Mn, SiO_2, As, etc., as in fig. 6), giving information on the deep circulation in the reservoir (ING unpublished data; Andreis, 1998; Danese, 1998).

The mineralized springs located along the Giudicarie Line are ferruginous, but at the same time have a very low electrical conductivity (oligo-mineral springs) with the exception of the Bagni di Mezzo (TAL 28-54). This spring is

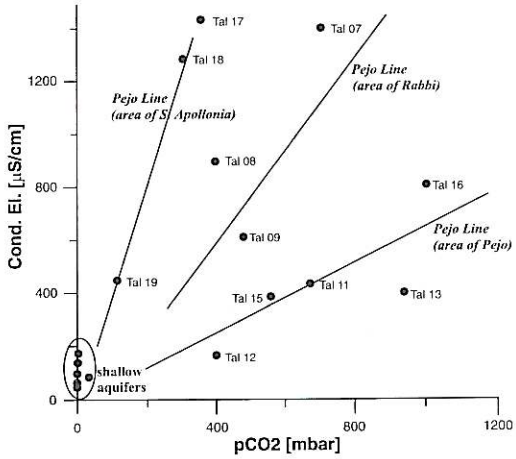

Fig. 6. pCO_2 *versus* electrical conductivity diagram, for the Pejo Line groundwater.

clearly different from the other Giudicarie Line samples: its high salinity and relatively high trace elements content (As, Fe, Mn, B, Li, SiO_2, etc.), as well as the low pH (4.59) suggested the deepening of the groundwater circuit. We calculated a reservoir temperature around 100 °C (Solmineq88 code). The high calculated pCO_2 and the high ^{222}Rn content deserve special interest as a consequence of the location of the spring at the confluence of the Pejo Line and Giudicarie Line, over a high fractured fault zone.

The northern and southern Giudicarie Line exhibit typically earth-alkaline bicarbonate groundwater; the same situation occurs for the Slingia Line, for the Braulio Line and for the Val Trafoi spring (TAL 23).

Otherwise, the Bagni di Mezzo, the S. Antonio and the Cinglaccia-Bormio springs have a Ca-SO_4 signature as a consequence either of the sulfide weathering (with H_2SO_4 production and pH lowering) or to the H_2S-SO_4 deep input.

The binary diagrams in figs. 7 and 8 show the relationships between ^{222}Rn and salinity as well as redox potential conditions of the aquifers, allowing immediate discrimination of the shallow groundwater circulation from the deep one along fault systems. More specifically, they distinguish three sectors along the Pejo Line (S. Apollonia, Pejo and Rabbi sectors), following

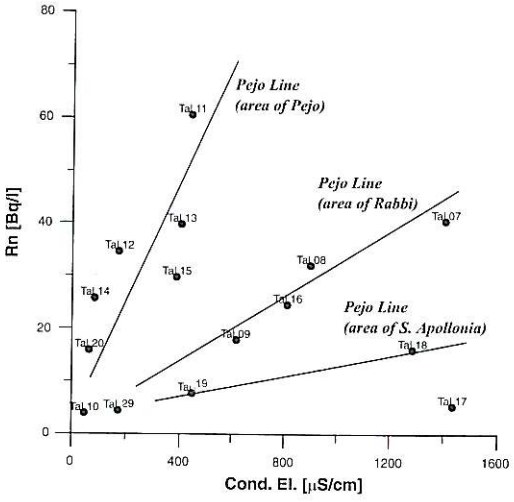

Fig. 7. Rn *versus* electrical conductivity diagram, for the Pejo Line groundwater.

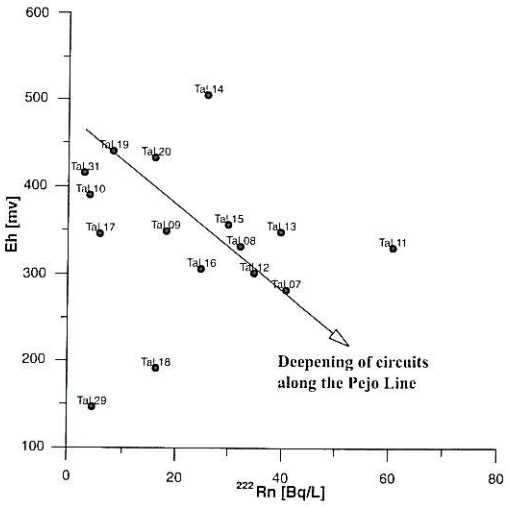

Fig. 8. Rn *versus* Eh (redox potential) diagram, for the Pejo Line groundwater.

the trends discovered with the pCO_2 - electrical conductivity diagram (fig. 6). The correlation between CO_2 and the ^{222}Rn enrichment (fig. 9) along the Pejo Line suggested a carrier role played by the CO_2 along this tectonic line. Our $\delta^{13}C$ data of the Fonte Antica Rabbi (TAL 7) suggested a thermo-metamorphic origin component of the CO_2 (ING not yet published data).

Along the confluence between the Giudicarie Line and the Pejo Line we found the highest values of ^{222}Rn content (one of the highest ^{222}Rn values found in Europe): 2002 Bq/L at the San Vigilio spring (TAL 26, 27, 52), although the low salinity of the spring, and 1929 Bq/L the Bagni di Mezzo spring (TAL 28-54) as abovementioned. In general, the Giudicarie Line springs showed a lower radon content with respect to the ferruginous-mineralized springs of the Pejo Line.

The Cinglaccia-Bormio thermal spring (38.3 °C) showed a very high ^{222}Rn content (TAL 21-49 with 970 Bq/L and 540 Bq/L, respectively), suggesting the existence of a deep groundwater circuit, closed to the CO_2 gaseous input. This deep circulation evolved inside the Ortles crystalline basement, tectonically in contact with

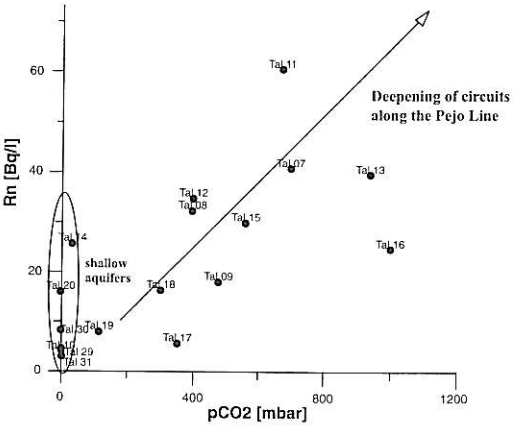

Fig. 9. Rn *versus* CO_2 partial pressure diagram, for the Pejo Line groundwater.

the sedimentary Ortles covers, from which the spring is up-welling along the Gran Zebrù Line. As a consequence of the convection established, with a rapid ascent (the difference between the reservoir temperature and the emergence temperature is only 20 °C), radon enrichment was

observed with respect to the shallow groundwater of the same area.

Therefore, the main difference between the springs located along the Giudicarie - Gran Zebrù and Slingia lines with respect those located along the Pejo Line is that in the former the radon enrichment was linked to the groundwater deepening, while in the latter the radon increase was linked to the CO_2 gas carrier input.

The inter-comparison between the CTM-ACC and ASM-LCC radon measurement methods for Eastern Alps groundwater (fig. 10), shows that the results obtained with the CTM are not in a good agreement with those obtained by the ASM-LCC method. The ASM-LCC/GSM-CTM ratio (figs. 10 to 13) was between 0.26 and 0.65, while un-common exception were samples TAL 47, TAL 50, TAL 50 and TAL 53. This peculiar un-correlation was found during the first Gargano sampling survey: perhaps the lack of a full gurgling (minor efficiency of the diffusive filter) inside the RU200 cylinder may have been the cause of the observed discrepancy for the Eastern Alps survey. So finally, the ASM-LCC results averaged about 45% of the CTM-ACC values.

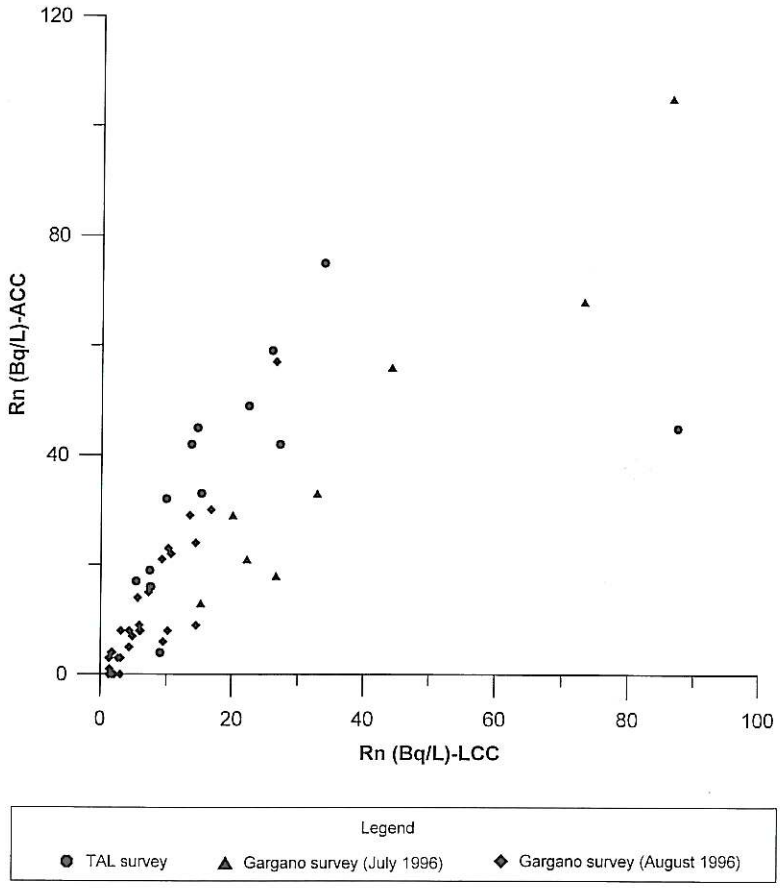

Fig. 10. Comparison between Rn values measured with ASM-LCC and GSM-CTM methods, throughout the Gargano and Eastern Alps (1996-1997 ING surveys); for a better comprehension of the diagram, values of TAL 49 (1505 by CTM 539 by ASM-LCC) and TAL 52 (3280 by CTM, 861 by ASM-LCC) are not reported.